Distributed Control to Ensure Proportional Load Sharing and Improve Voltage Regulation in Low-Voltage DC Microgrids

Anand, Sandeep; G. Fernandes, Baylon; Guerrero, Josep M.

Published in:
I E E E Transactions on Power Electronics

DOI (link to publication from Publisher):
10.1109/TPEL.2012.2215055

Publication date:
2013

Document Version
Early version, also known as pre-print

Distributed Control to Ensure Proportional Load Sharing and Improve Voltage Regulation in Low Voltage DC Microgrids

Sandeep Anand[(1)], Baylon G. Fernandes[(1)] and Josep M. Guerrero[(2)]

[(1)]Electrical Engineering Department, Indian Institute of Technology Bombay, India
[(2)] Institute of Energy Technology, Aalborg University, Denmark
Email: sa@ee.iitb.ac.in, bgf@ee.iitb.ac.in, joz@et.aau.dk

Abstract

DC microgrids are gaining popularity due to high efficiency, high reliability and easy interconnection of renewable sources as compared to ac system. Control objectives of dc microgrid are: (i) ensure equal load sharing (in per unit) among sources and (ii) maintain low voltage regulation of the system. Conventional droop controllers are not effective in achieving both the aforementioned objectives simultaneously. Reasons for this are identified to be the error in nominal voltages and load distribution. Though centralized controller achieves these objectives, it requires high speed communication and offers less reliability due to single point of failure. To address these limitations, this paper proposes a new decentralized controller for dc microgrid. Key advantages are high reliability, low voltage regulation and equal load sharing, utilizing low bandwidth communication. To evaluate the dynamic performance, mathematical model of the scheme is derived. Stability of the system is evaluated by eigenvalue analysis. The effectiveness of the scheme is verified through detailed simulation study. To confirm the viability of the scheme, experimental studies are carried out on a laboratory prototype developed for this purpose. Controller Area Network (CAN) protocol is utilized to achieve communication between the sources.

Index Terms - DC Microgrid, Droop Controller, Load Sharing, Stability Analysis.

1 Introduction

Distributed power generation systems, comprising small generation and storage units, are gaining popularity due to increasing energy demand. Low distribution losses, high reliability, reduced chances of blackout, easy scalability and remote electrification are the key advantages of the distributed systems. Microgrid includes the control and coordination of distributed generation and storage units to maintain power balance between sources and loads.

In the recent years, depleting fossil fuels, ever-increasing energy demand and concern over climate change, necessitate a substantial percentage of the power to be generated by renewable sources. However, supplying electronic loads, variable speed drives and LED loads from renewable sources require multiple ac-dc and dc-ac conversions [1]. This causes substantial energy wastage before end use. To address this limitation, dc system is suggested, which offers high efficiency and reliability [1–7].

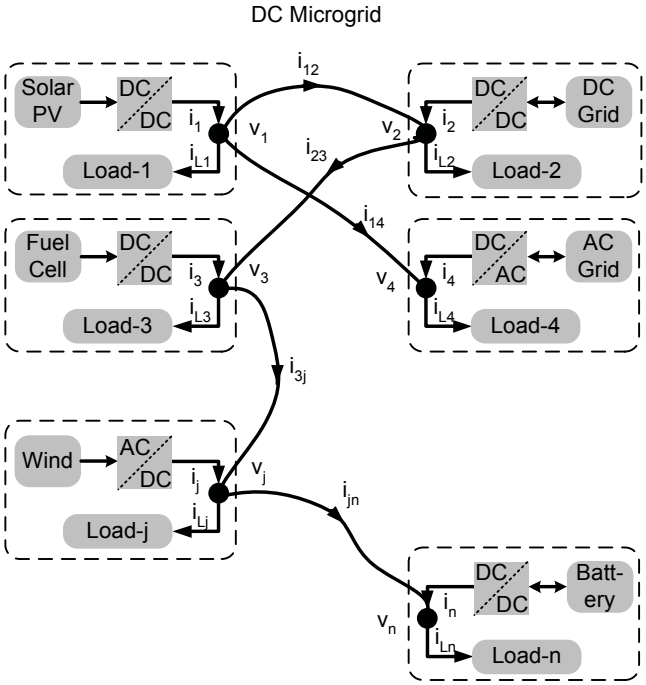

Figure 1: Generic dc microgrid

A generic dc microgrid integrating various sources and loads is shown in Fig. 1. The generic microgrid structure enables interconnection of any sources within the microgrid. DC microgrid can be connected to the ac main grid by an ac-dc converter with bidirectional power flow capability or to a dc electrical distribution network. To interconnect sources and storage elements of dissimilar electrical characteristics, power electronics converters (PEC) (such as ac-dc, dc-dc etc) are included between each source/storage and the microgrid.

Sources and storage elements are controlled to supply high reliability power to loads. Hierarchy of controllers for microgrid is reported in [8]. Similar structure for dc microgrid is shown in Fig. 2. Tertiary control, also known as energy management system, communicates with the Distribution System Operator (DSO) or Transmission System Operator (TSO) and the secondary control. DSO/TSO decides the schedule of power exchange with the microgrid. Based on this and other inputs from within the microgrid, the tertiary controller prepares the source and storage dispatch schedule. This is communicated to the secondary controller. Secondary controller's objective is to ensure that the power supplied by different sources is in proportion to that scheduled (base value) by the tertiary control. In other words, load must be shared proportionally (in per unit) among sources. Typically, both secondary and tertiary controls are included in the Microgrid Central Controller (MGCC). Secondary control sets the parameters of droop (primary) control such that deviations produced by the droop control are restored and the dc microgrid voltage is maintained within the acceptable values. Objective of the droop control is to compensate for instantaneous mismatch between scheduled power and power demanded by loads. Based on these requirements, droop control generates the voltage reference signals for source. Inner loop (voltage and current) control, ensure that the actual voltage of PEC source is equal to its reference value.

For communication between DSO/TSO and the microgrids, Local Area Network (LAN) / internet can be used [9]. But infrastructure for this communication technique may not be available at remote locations. Therefore, use of these techniques for communication within the microgrid, between secondary and primary controllers, may not be viable. Additional investment is required to realize this communication method. Use of Power Line Communication (PLC) is becoming popular for control of ac electrical systems [10]. Study on the viability of PLC for low voltage dc system is reported in [11]. DC microgrid can have various interconnections of power cables, thereby making the analysis of channel complex [12]. Another suitable technique for communication within the microgrid is Controller Area Network (CAN) [13, 14]. Typically, digital signal processors / controllers used for power electronics applications, include CAN protocol, thereby facilitating CAN communication among these devices.

Design and implementation issues of voltage and current controllers for ac-dc and dc-dc converters are reported in [15, 16]. Further, tertiary control, which decides the dispatch schedule within the microgrid, is almost the same for ac and dc microgrid. Therefore, existing literature on energy management systems for ac microgrids [17–20] can be suitably adapted for the dc mi-

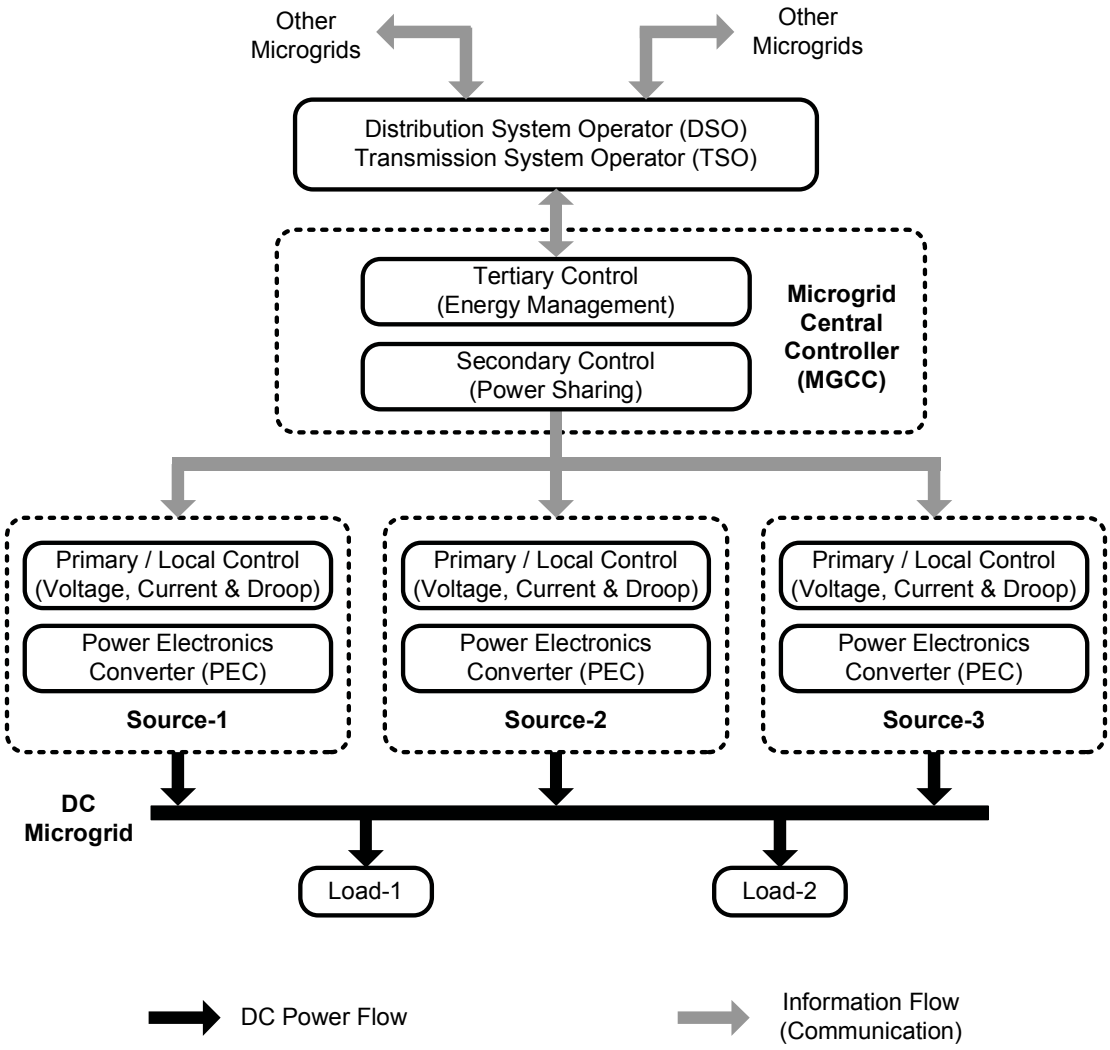

Figure 2: Hierarchical control of dc microgrid

crogrid. However, the secondary control, which ensures power sharing among sources, depends on the characteristics of power flow within the microgrid network. For large ac systems, real power flow depends on the difference between the voltage phase angles across the transmission line. However, real power flow in a dc system depends on the difference of voltage magnitude across the cable. Further, at steady state, frequency of ac voltage is same throughout the system, while in dc system there is no such parameter which remains same throughout. Due to these significant differences, secondary control of ac microgrid cannot be used for dc microgrid. Separate study of dc microgrid is required to identify the suitable power sharing control.

In [21] a droop controlled superconductive dc system catering to a small zone is analyzed. Effect of interconnecting cable resistance is neglected in the dc systems. It may be noted that this effect becomes significant for low voltage dc system. A power management strategy for dc system in More Electric Aircraft (MEA) is given in [22]. This method assumes a centralized

generator and does not address the issues pertaining to unequal load sharing in distributed sources. Analysis on the effect of interconnecting cable given in [23] is limited to one source, one load system. Therefore, it does not demonstrates the effect of unequal load sharing in distributed generation system. Control of distributed generation system suggested in [24–26] utilize the system voltage level as a means of communication. PECs connected to microgrid measure the system voltage level and accordingly set reference value for operation. However, voltage level at different locations vary due to resistive drop across the interconnecting cables. Therefore, use of this control scheme is limited to small systems, in which resistance drops can be neglected. To address this limitation a small ac signal over the dc signal is injected in the method reported in [27, 28]. The frequency of this ac signal acts as a means of communication. This method is prone to noise on power cables. Further, it requires circuits for accurate injection and detection of the ac signal. This limits the viability of the scheme.

To address the aforementioned limitations, a distributed control to ensure proportional load sharing in low voltage dc microgrid is proposed in this paper. The control uses low bandwidth communication for improved voltage regulation as compared to that in conventional droop control. In addition, the proposed scheme offers high reliability as compared to the centralized control.

Section-II compares usability of different controllers to achieve load sharing. Primary factors affecting the performance of droop controlled dc microgrid are explained. Section-III describes the proposed decentralized control scheme using low bandwidth communication. Stability is evaluated based on the derived dynamic model of the dc microgrid. To verify the operation of the proposed scheme, detailed simulation and experimental studies are conducted and results are included in Section-IV. Section-V concludes the paper.

2 Distributed Control Architectures

The main objectives of the power sharing control is to maintain low voltage regulation without compromising the load sharing (in per unit) among the sources. This control can be classified into three categories:

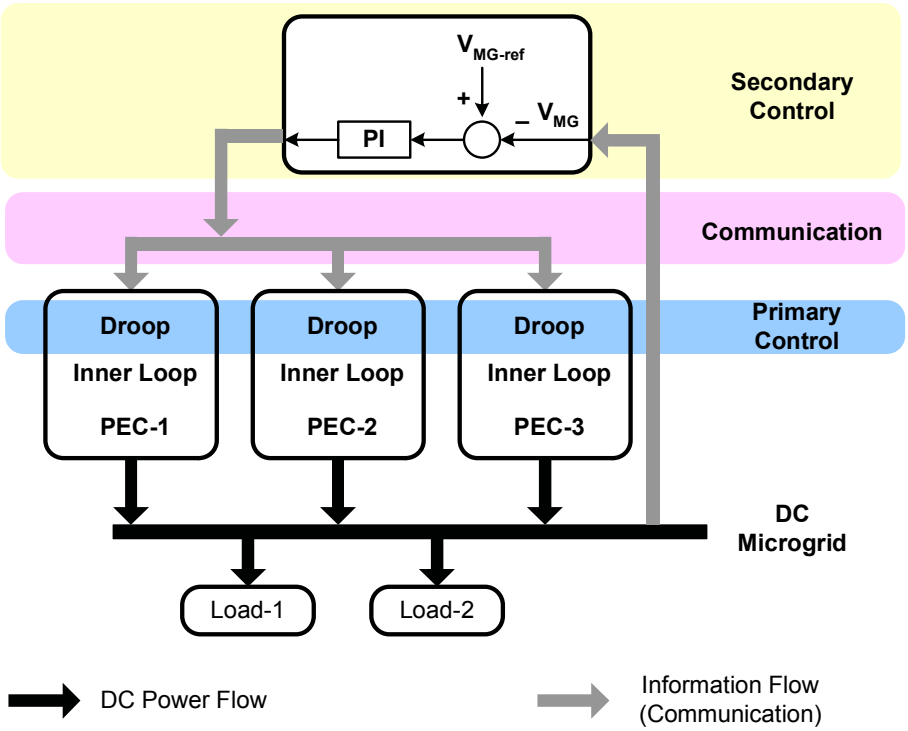

Figure 3: Centralized secondary control in hierarchical control scheme [8]

2.1 Hierarchical Control

A centralized power sharing (secondary) control scheme for dc microgrid, given in [8] is shown in Fig. 2. Each PEC source includes a primary (droop) control and inner (voltage and current) control. Secondary control is centralized and is responsible for controlling various primary controllers. Secondary control sets parameters for the droop law of each PEC source. Fig. 3 shows the secondary and primary controllers for the hierarchical control scheme. Voltage level of the microgrid is compared with the reference value and this error is processed through the Proportion-Integral (PI) controller. Output of the PI is communicated to primary control of all sources. This scheme achieves low voltage regulation. Furthermore, distributed primary control ensures that system operation is not effected by malfunction of a source. However, in case of failure of the secondary control, the system may not be able to ensure low voltage regulation.

2.2 Control Without Communication

Decentralized control without communication is shown in Fig. 4 [21, 29]. It comprises of droop control and does not include a separate secondary control unit. For dc systems, droop between

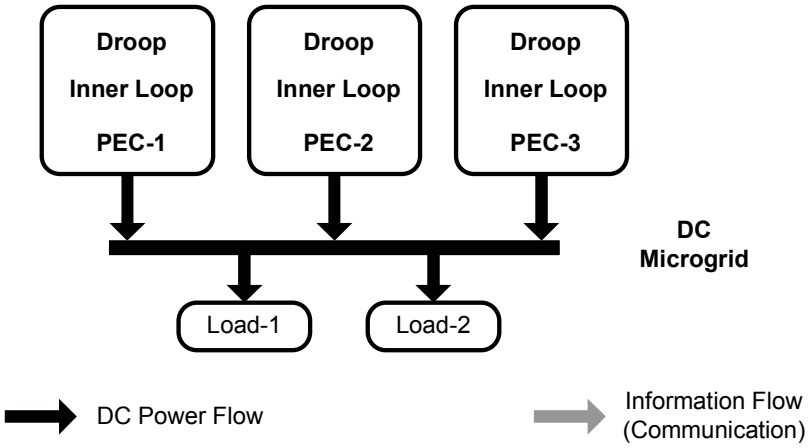

Figure 4: Control of dc microgrid without communication

voltage and current is most commonly used and is given by:

$$v_j^{ref} = v_j^0 - d_j i_j \tag{1}$$

where, d_j, i_j, v_j^{ref} and v_j^0 are the droop gain, source current, reference voltage and nominal voltage (voltage when source current is zero) of source-j respectively. Since secondary control is not used, parameters of the droop control are set such that system voltage is maintained within the specified value. Therefore, to ensure low voltage regulation, low value of droop gain, d_j is used. This control scheme offers complete modularity at less cost as compared to the hierarchical control. However, error in power sharing among sources is high as compared to that in hierarchical control. Following are the two reasons for error in power sharing in droop controlled system without communication:

2.2.1 Unequal Nominal Voltages

Due to limitations in implementation of primary controllers, the nominal voltages of different PEC sources are not exactly equal. Typically, this is due to error in voltage sensing for closed loop operation. Small error in nominal voltages results in significant deviation of source currents from their required values. This is due to the small value of the droop gain used to restrict large variation in system voltage (between no-load and full-load conditions). For two parallel connected dc sources, unequal load sharing due to small error in nominal voltages is shown in Fig. 5. In case of small droop gain the deviation in source current, $(i_1 - i_2)$ is large. As the droop gain is increased, $(i_1 - i_2)$ reduces. However, the voltage regulation is large and may not be acceptable to loads. Similar problem of unequal load sharing for parallel connected dc

converters is discussed in [30].

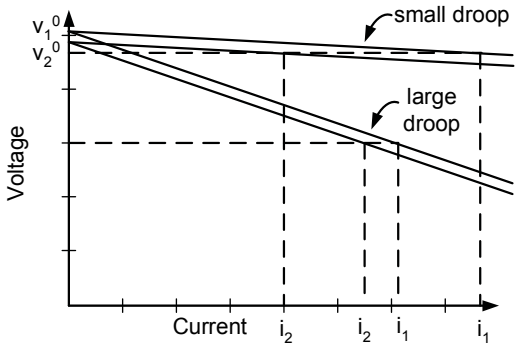

Figure 5: Unequal load sharing due to error in nominal voltages of two parallel connected dc converters.

2.2.2 Load Distribution

In dc microgrid, difference in voltage magnitudes of two nodes vary with the power flow across their interconnecting cables. In other words, voltage of each node depends on the load distribution across the system. Due to droop control, source currents depend on the node voltages. Therefore, source currents depend on the load distribution due to the interconnecting cable resistance. Increasing the droop gains results in less deviation of source currents. This is at the cost of increased voltage variation. To further demonstrate this, a two source and two load system, shown in Fig. 6, is analyzed. Source-1 and 2 are interconnected by a cable, which is modeled as resistance for steady state analysis and series combination of resistance and inductance for stability analysis. Both sources have local loads. Source-1 and 2 are of equal rating, thus have same droop gain, d. Details of the system parameters are given in Table-1.

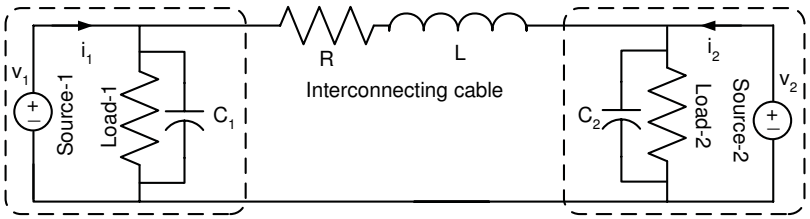

Figure 6: A two source, two load dc microgrid

Steady state equivalent circuits of the microgrid, with sources represented in thevenin and norton forms are shown in Fig. 7. Consider load-1 is off, load-2 is drawing rated current and system has reached steady state. Voltage-current characteristics for both sources as seen by load-2 are given in Fig. 8. Y-axis represents the voltage across load-2 and X-axis represents

Table 1: Parameters of two node dc microgrid

Parameters	Value (units)
Nominal Voltage	48V
Rated power (each source)	250W
Required voltage regulation	<5%
Cable Resistance, R	205mΩ
Cable Inductance, L	463μH
Load-2 impedance	6Ω

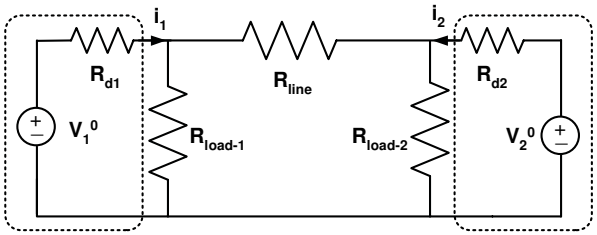

(a) Thevenin Equivalent Circuit

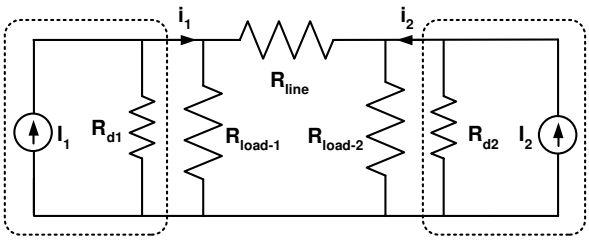

(b) Norton Equivalent Circuit

Figure 7: Steady state equivalent circuit of dc microgrid in (a) Thevenin form and (b) Norton form.

the currents drawn from source-1 and source-2. Slope of the characteristics is the addition of droop gain and the total resistance from source to load. For droop gains, R_{d1} and R_{d2} equal to 0.276Ω (comparable to the cable resistance), currents supplied by source-1 and source-2 are 3A and 5A respectively. Deviation in currents drawn from their ideal values (4A) is 25%. Voltage regulation (between no-load and full-load) is 2.9% of the nominal. This shows that, low values of droop gain ensure good voltage regulation, but load sharing performance is unacceptable. For high value of droop gain, $R_{d1} = R_{d2} = 1.9\Omega$ as shown in Fig. 8, currents drawn from source-1 and source-2 are 3.8A and 4.2A. Deviation in currents from their ideal values is 5%, which is significantly lower than the previous case. However, voltage regulation has increased to 16.6%, which may not be acceptable for the loads. Therefore, presence of interconnecting cable resistance introduces tradeoff between load sharing and voltage regulation.

In summary, use of droop control without communication are not effective in low voltage dc microgrid due to (i) unequal nominal voltages and (ii) load distribution. For low value of droop

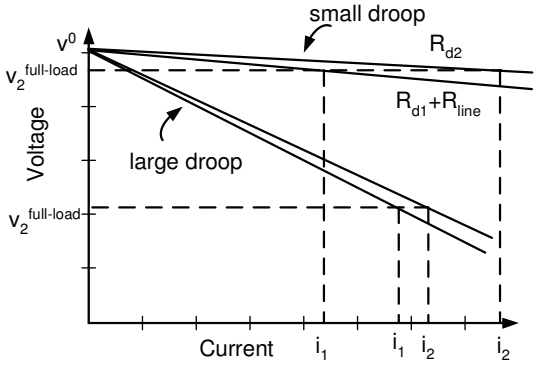

Figure 8: Unequal load sharing due to load distribution in dc microgrid

gain, these factors deteriorate load sharing among the PEC sources. Though, for large droop gains better load sharing is achieved, voltage deviation of the dc microgrid may be unacceptable.

In ac systems, droop between active power and frequency is incorporated to achieve sharing of (active) power among sources [31–35]. At steady state, frequency of the voltage is same throughout the system, thereby ensuring that active power is shared proportionally among the sources. However, in case of large resistive line, tradeoff exists between higher feedback gain for better power sharing and system stability [9]. Therefore, performance deteriorates and additional control using communication is required [9]. For reactive power sharing, droop between reactive power and voltage magnitude is used. However, since the voltage magnitude vary within the microgrid, proportional reactive power sharing is not achieved [36]. A solution by injecting signals in the ac system is suggested in [37]. The injected signal acts as a means of communication among sources.

The problem of power sharing in dc microgrid, presented in this paper is similar to that of reactive power sharing in inductive-line ac microgrids [36] and active power sharing in resistive-line ac microgrid [9].

2.3 Distributed Control for Parallel DC-DC Converters

A distributed control scheme utilizing the average current sharing (ACS) [38] is shown in Fig. 9. Instead of a single secondary control, distributed control is incorporated in each PEC source. These controllers communicates to each other using a common bus. Average Current Sharing (ACS) control of parallel dc-dc converters suggested in [38] is shown in Fig. 10. The droop controller consists of V_0^{ref} and $d1$. Measured value of source current is converted to voltage signal, which is connected to the average current sharing bus (analog) through a resistance, R_1.

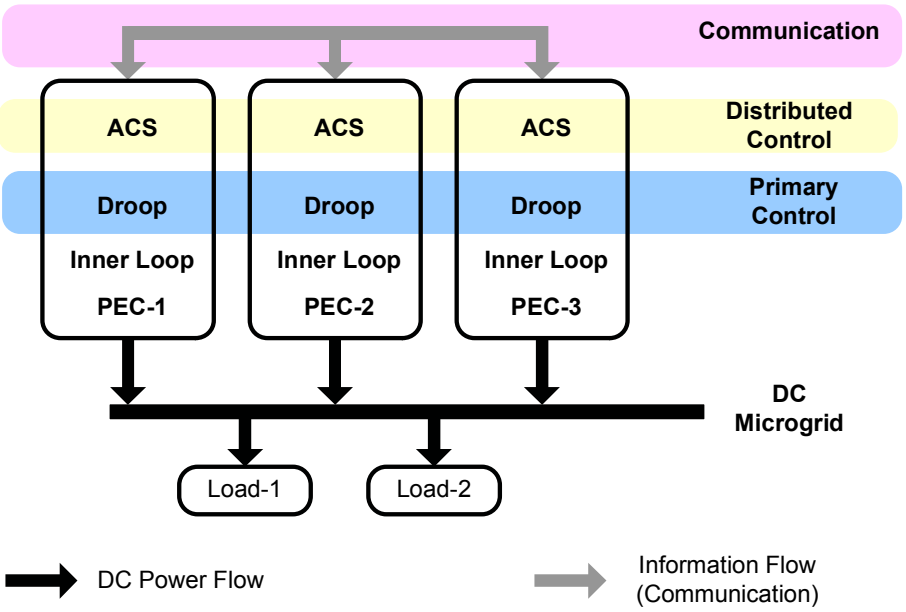

Figure 9: Distributed control for dc microgrid

If resistance R_1, R_2, $\cdots$, R_n are equal, voltage appearing on the bus corresponds to $\sum i/n$. This signal is added to the droop control. This scheme offers equal load sharing among sources and low voltage regulation in parallel dc-dc converter system. In dc microgrid, sources are distributed over a region. The current sharing bus has to be distributed within the region along with power lines. This may inject significant external noise in the bus. Therefore, this scheme may not be suitable for dc microgrid.

Table 2: Comparison of control architectures for dc microgrid

Control	**Voltage Regulation**	**Load Sharing**	**Modularity**
Secondary (Hierarchical)	Precise	Intermediate	Low
Droop (without communication)	Good	Inaccurate	High
Distributed	Good	Precise	High

To summarize, comparison of the aforementioned control architectures for dc microgrid application is shown in Table-2. The hierarchical scheme offers precise voltage regulation and intermediate load sharing performance. However, modularity is low due to single secondary control. Though, droop control (without communication) offers high modularity, load sharing performance is unacceptable. Distributed control ensures good voltage regulation along with precise load sharing. Moreover, it offers better modularity as compared to that of hierarchical control. In this paper, a digital distributed control suitable for dc microgrids is proposed.

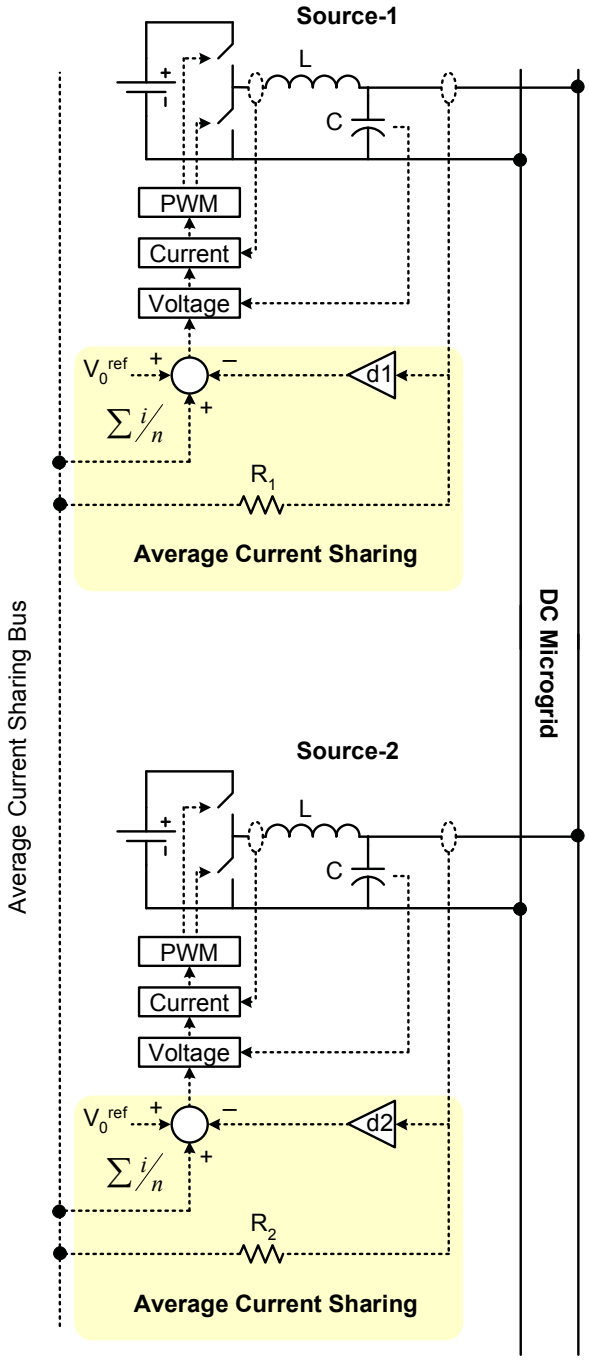

Figure 10: Average current sharing control for parallel dc-dc converters [38]

3 Proposed Distributed Control

As discussed in Section-2.2, for conventional droop controllers, low value of droop gain ensures low voltage regulation. But the source currents deviate significantly from their ideal values and equal load sharing cannot be guaranteed. The factors for this behavior are unequal nominal voltages and load distribution. Though these issues can be addressed by increasing the droop gains higher than the cable resistance, voltage of the system vary significantly from no-load to

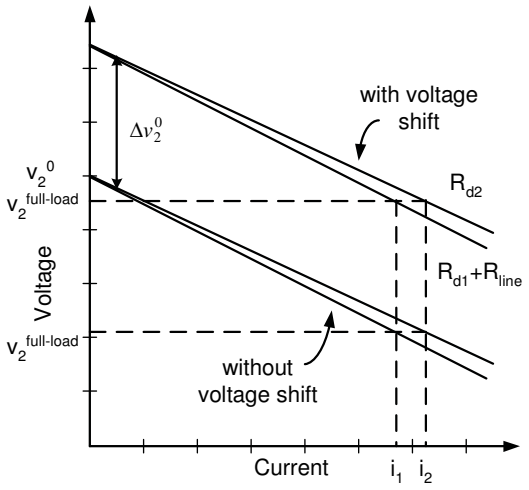

Figure 11: Droop characteristics for large droop gain with voltage shifting

full-load condition. Following scheme is proposed to address this limitation.

Droop characteristics is shifted along the voltage axis by addition of Δv_j^0 in the conventional droop equation and is given by:

$$v_j^{ref} = v_j^0 + \Delta v_j^0 - d_j i_j \tag{2}$$

Shift in the voltage, Δv_j^0 depends on the total system load. With increase in load, Δv_j^0 increases, making the instantaneous voltage reference, v_j^{ref} close to the nominal voltage, v_j^0. For the dc microgrid shown in Fig. 6, both source characteristics shift. Characteristics before and after shifting observed at load-1 is shown in Fig. 11. Even though high value of droop gain is used to ensure equal load sharing, operating voltage is close to the nominal voltage, v_j^0. To determine the value of voltage shift, Δv_j^0 a low bandwidth communication is utilized as follows: The controller of each source communicates with the controller of other sources and sends the magnitude of current supplied (in per unit) by it. Using this information the individual source controller determines the average value of the current supplied by all the sources using,

$$i_j^{avg} = \frac{\Sigma_{m=1}^{n} i_m^{pu}}{n} \tag{3}$$

where, i_m^{pu} is the source-m current in per unit. Shift in droop of each source is set according to their calculated average current as follows:

$$\Delta v_j^0 = k_j i_j^{avg} i_j^{rated} \tag{4}$$

where, k_j and i_j^{rated} are the shift gain and rated current of source-j respectively. For change in load, sources continue to share the demanded power equally due to large droop gains. Instantaneously system voltage as given by (2) may vary from its nominal value due to the change in source current. It is restored once the new values of currents are communicated among sources and new value of voltage shifts, Δv_j^0 are calculated. This shift control is termed as Digital Average Current Sharing (DACS) control. The control circuit diagram including the droop and shift controllers (DACS) is shown in Fig. 12.

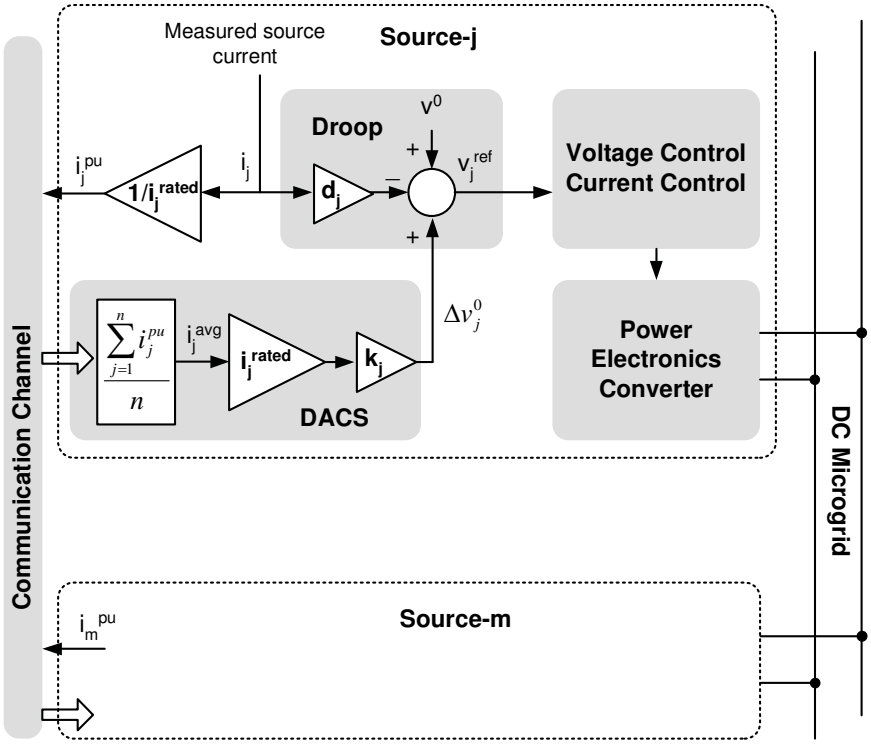

Figure 12: Proposed distributed control

3.1 Selection of droop gain, d_j

Steady state model of the dc microgrid controlled by droop controller is developed in [2]. The deviation in source currents from their ideal values due to error in nominal voltages and load distribution are given by the following equation.

$$\left(\mathbf{M^T R^{-1} M D + E_{n\times n}}\right)\mathbf{\Delta I} = \mathbf{M^T R^{-1} M V^0} + \mathbf{\Delta I_L} \tag{5}$$

where, $\mathbf{M}$, $\mathbf{R}$, $\mathbf{D}$ and $\mathbf{E_{n\times n}}$ are incidence matrix of the network, resistance matrix, droop matrix and identity matrix respectively. $\mathbf{V^0}$ and $\mathbf{\Delta I_L}$ are vectors representing nominal voltages and deviation in load currents. The total deviation in source currents from their ideal values is

ΔI. By substituting the system parameters and the required source current deviations in (5), suitable value of droop gains are determined. Typically, to limit the current deviations to a low values, large droop gains are required. This leads to large voltage regulation problem. This is addressed by suitably selecting the shift gains.

3.2 Selection of shift gain, k_j

The value of shift gain, k_j is determined based on the following criteria:

1. Value of shift, Δv_j^0 should be as close as possible to the product of droop gain and source current, $d_j i_j$. This ensures that the voltage drop due to droop is compensated by the appropriate shift in the nominal voltage. Hence, operating voltage is close to the nominal voltage of the system.

2. Droop characteristics of all the sources should shift by the same amount. This is to ensure the shifting does not effect the load sharing. Therefore, product of shift gain, k_j and rated current, i_j^{rated} should be same for all sources.

$$k_1 i_1^{rated} = \cdots = k_j i_j^{rated} = \cdots = k_n i_n^{rated} \tag{6}$$

3. When only one source is operational, equation (3) shows that average current, i_j^{avg} is equal to source current, i_j^{pu}. Substituting this in equation (4) gives, shift in voltage, Δv_j^0 is equal to $k_j i_j$. Therefore, the resultant control equation (2) simplifies to

$$v_j^{ref} = v_j^0 - (d_j - k_j)\, i_j \tag{7}$$

   For stable operation the resultant slope, $(d_j - k_j)$ should be greater or equal to zero. Therefore, shift gain should be smaller than droop gain for stable operation.

$$k_j \leq d_j \quad \forall \quad 1 \leq j \leq n \tag{8}$$

3.3 Steady State Performance

The steady state performance of the proposed scheme is analytically evaluated for the system shown in Fig. 6. Details of the system parameters are given in Table-1. Load-2 is drawing its rated current and load-1 is turned off. Droop gains, $d_1 = d_2 = 1.9\Omega$, are much higher than

the cable resistance. Further shift gains, $k_1 = k_2 = 1.8\Omega$ are selected based on the criteria mentioned above. Currents drawn from source-1 and source-2 are 3.8A and 4.2A respectively. Deviation in currents from their ideal value is 5%. Further, voltage regulation is 1.62% between no-load and full-load. Both current deviation and voltage regulation are within the acceptable values. This shows good steady state performance of the proposed scheme.

3.4 Dynamic Stability

DC microgrid, including the proposed controller, is modeled to determine the stability. It is assumed that voltage control limits the bandwidth of the droop control. Hence, while analyzing the microgrid structure and droop controllers, fast dynamics are neglected by assuming the output voltage, v_j equal to its reference value, v_j^{ref}. Further, sampling and updating rate of the shift, Δv_j^0 is much slower than the droop controller. Therefore, the dynamics associated with the shifting algorithm do not effect the stability of the droop controlled system. Based on these two assumptions the small signal model of the system is derived. Important steps of derivation are included in the appendix and the derived model is given below:

$$\frac{d\hat{\mathbf{x}}}{dt} = \mathbf{A}\hat{\mathbf{x}} + \mathbf{B}\hat{\mathbf{u}} \tag{9}$$

where,

$$\hat{\mathbf{x}} = \begin{pmatrix} \hat{\mathbf{i}}_{\mathbf{xy}} \\ \hat{\mathbf{v}} \end{pmatrix} \tag{10}$$

$$\hat{\mathbf{u}} = \hat{\mathbf{p}}_{\mathbf{L}} \tag{11}$$

$$\mathbf{A} = \begin{pmatrix} -\mathbf{L}^{-1}\mathbf{R} & \mathbf{L}^{-1}\mathbf{M} \\ -\mathbf{C}^{-1}\mathbf{M}^{\mathbf{T}} & -\mathbf{C}^{-1}\mathbf{D}^{-1} + \mathbf{C}^{-1}\mathbf{V}^{-1}\mathbf{I}_{\mathbf{L}} \end{pmatrix} \tag{12}$$

$$\mathbf{B} = \begin{pmatrix} \mathbf{N}_{\mathbf{mxn}} \\ -\mathbf{C}^{-1}\mathbf{V}^{-1} \end{pmatrix} \tag{13}$$

where, $\hat{\mathbf{i}}_{\mathbf{xy}}$, $\hat{\mathbf{v}}$ and $\hat{\mathbf{p}}_{\mathbf{L}}$ are vectors representing small signal variation in interconnecting cable currents, source voltages and load powers respectively. Definition of the other symbols used is given in appendix. From this model, eigenvalues for the system given in Table-1 are found to be:

$$\lambda_1 = -443 - 2076j$$
$$\lambda_2 = -443 + 2076j$$
$$\lambda_3 = -443 \tag{14}$$

Real part of all the eigenvalues are negative, which indicates stable operation of the system. Further, to determine the effect of interconnecting cable parameters, root locus plot are shown in Fig. 13 and 14. Variation of system eigenvalues with increasing inductance, L and resistance, R are shown in Fig. 13 and Fig. 14 respectively. Both inductance and resistance values are increased from 50% to 200% of their base values given in Table-1. Eigenvalues move towards the +ve real plane with increase in inductance, thereby reducing the stability margin. However, with higher resistance, system becomes more stable.

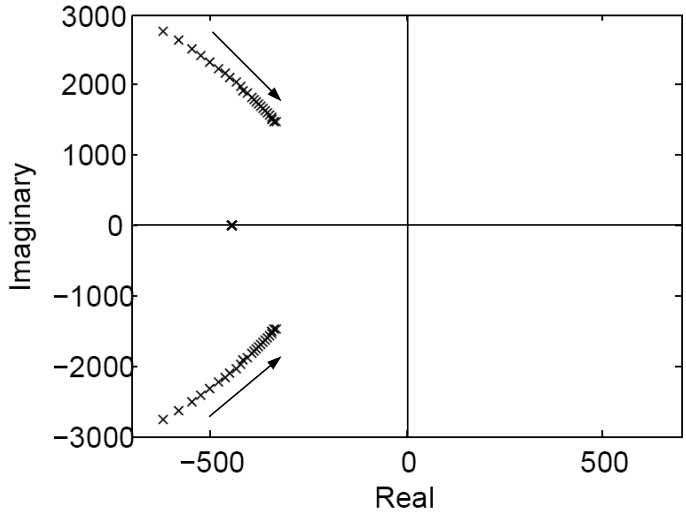

Figure 13: Root locus of system eigenvalues for increasing cable inductance, L

3.5 Communication Requirements

The control technique proposed in this paper requires digital communication among sources for its operation. In the proposed control scheme only output current value of each source is shared. This requires transmission of only two byte data by each source. Total data transmitted over the

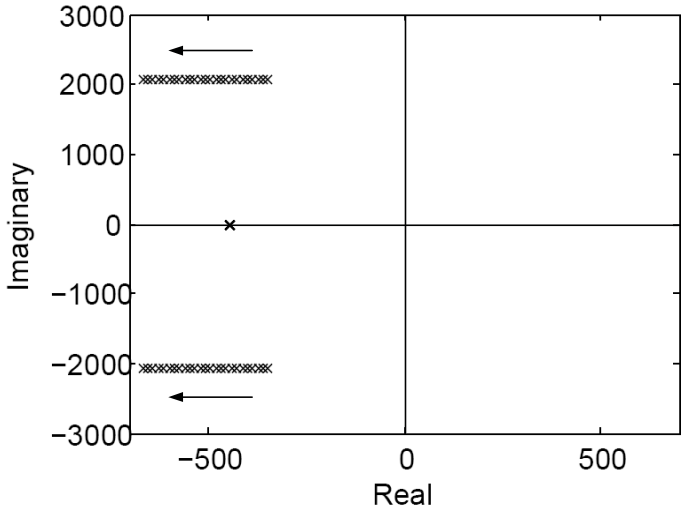

Figure 14: Root locus of system eigenvalues for increasing cable resistance, R

communication channel is $2n$ bytes, where n is the number of sources. Data read by each source is $2(n-1)$ bytes. Hence, communication technique has to manage small data packets. Further, the rate of transmitting the data is low, thereby making the use of low speed communication viable. Thus, controller area network (CAN) based low speed and low cost communication scheme is used.

4 Results And Discussion

4.1 Simulation

Two load, two source dc system shown in Fig. 6 is simulated using MATLAB/Simulink. Parameters used for simulation are given in Table-1. Each source is a dc-dc buck converter with inner voltage controller as shown in Fig. 15. The proposed controller is realized to generate the reference value of voltage for inner controller. Droop gains, $d_1 = d_2 = d$ are set to 1.9 for equal load sharing. Using the conditions given in section-3.2, the shift gain, $k_1 = k_2 = k$ are set to 1.8. Each source sends the magnitude of current supplied by it to the other source at every 10ms. Total delay in communication channel is around 0.1ms. To simulate the transient condition, load-2 is turned on. Output voltages of source-1 and source-2 on no-load are equal to 47.8V. After load-2 is turned on, the steady state voltage of source-1 and source-2 are 47.8V and 47.1V respectively. This corresponds to voltage regulation of 1.85%. Source-1 and 2 currents are 3.92A and 4.36A respectively. Ideally both currents should have been 4.14A. Deviation in source currents from their ideal value is 5.3%. This verifies good steady state performance

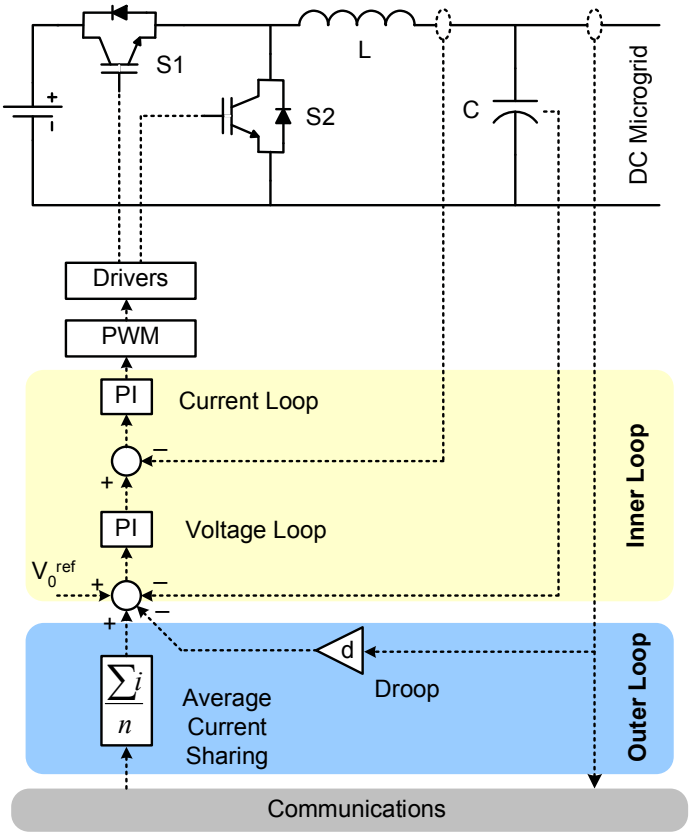

Figure 15: DC-DC buck converter with inner voltage control and outer control.

of the proposed scheme. Output voltages and currents of both sources, and voltage shifts are shown in Fig. 16. Voltage shifts, Δv_1^0 and Δv_2^0 are overlapping and increase with total load on the system, to compensate for drop due to droop controller. The new value of voltage shifts are calculated after every 10ms.

Further, simulation studies are carried out to determine the effect of interconnecting cable resistance, R and inductance, L. Simulations results are summarized in Table-3. Each row corresponds to a fixed value of inductance and each column corresponds to a fixed value of resistance. Other system parameters are kept same. Each entry in the table is (α,β), where α is the voltage regulation and β is the deviation in current sharing. It is observed, that variation in α and β is very small along a column. This implies that variation in inductance does not effect the steady state performance. However, interconnecting cable resistance has a direct effect on the current sharing among sources.

4.2 Experimental Setup

A laboratory prototype of microgrid, shown in Fig. 6, is developed. Both the sources are dc-dc buck converters of equal power rating. Each converter is controlled by the inner voltage

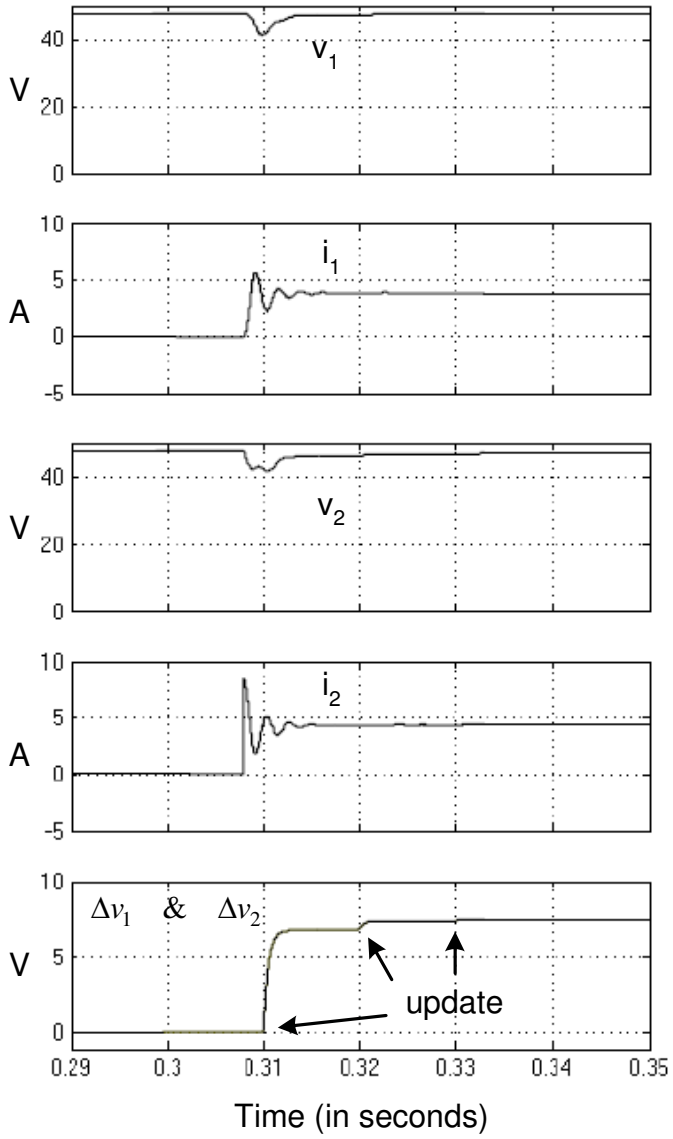

Figure 16: Simulation results. Source voltages, v_1 and v_2 (20V/div), source currents, i_1 and i_2 (5A/div) and voltage shifts, Δv_1^0 and Δv_2^0 (5V/div); X-axis: 10ms/div

Table 3: Voltage regulation and deviation in currents for different inductance and resistance.

	R=0.5×205mΩ	**R=1×205mΩ**	**R=2×205mΩ**
L=0.5×463μH	1.45%V/V, 2.82%A/A	1.85%V/V, 5.34%A/A	2.59%V/V,9.85%A/A
L=1×463μH	1.44%V/V, 2.84%A/A	**1.85%V/V, 5.28%A/A**	2.59%V/V, 9.9%A/A
L=2×463μH	1.45%V/V, 2.79%A/A	1.85%V/V, 5.35%A/A	2.59%V/V,9.9%A/A

controller as shown in Fig. 15. System parameters are given in Table-1. Both inner and outer control loops are realized using TMS320F28335 digital controllers.

By operating each converter separately at no-load, error between the reference and actual output voltage is observed to be less than 1%. This error is introduced by analog circuits used for attenuating the feedback signals. Further, 0.82V drop is expected across the interconnecting

cable due to current flow of 4A. This corresponds to 1.7% of the nominal voltage. Therefore, to achieve less than 5% regulation of system voltage, secondary controller should provide the reference voltage within 2.3% (=5-1-1.7) of the nominal value. Both conventional droop controller and the proposed distributed controller (droop + digital average current sharing) are realized such that aforementioned condition on reference voltage is met. Results obtained for these controllers are compared below:

4.2.1 Droop Method

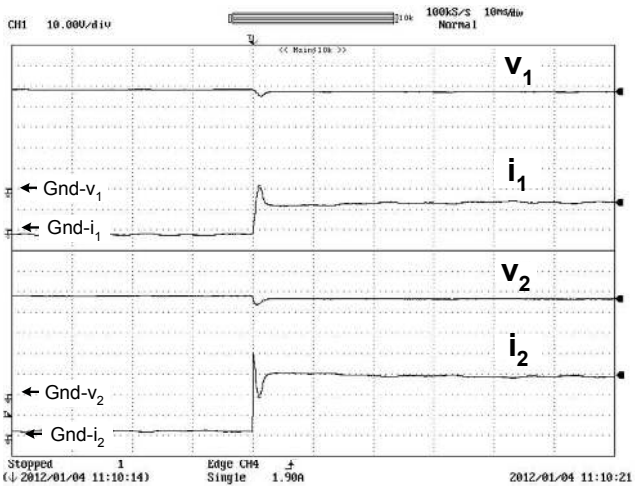

Figure 17: Experimentally obtained transient response for droop controller. Trace-1: Source-1 voltage (10V/div) and current (2A/div); Trace-2: Source-2 voltage (10V/div) and current (2A/div); X-axis: 10ms/div

To achieve system voltage regulation less than 5%, droop gain for the conventional droop controller is set to 0.276Ω for both converters. This value is comparable to the interconnecting cable resistance. Fig. 17 shows the transient results for step change in load-2 from zero to full-load (8.44A). The voltages of source-1 and 2 after loading are 47.70V and 47.28V respectively. These values correspond to the system voltage regulation of 1.5%, which is within the specified value. Currents supplied by source-1 and source-2 are found to be 2.71A and 5.73A respectively. Ideally, both source currents should be equal to 4.22A. Therefore, deviation in source currents from the ideal value is 35.8%.

4.2.2 Proposed Method

Digital average current sharing control, shown in Fig. 15 is realized using TMS320F28335 controller. Both sources communicates using Controller Area Network (CAN) protocol. CAN

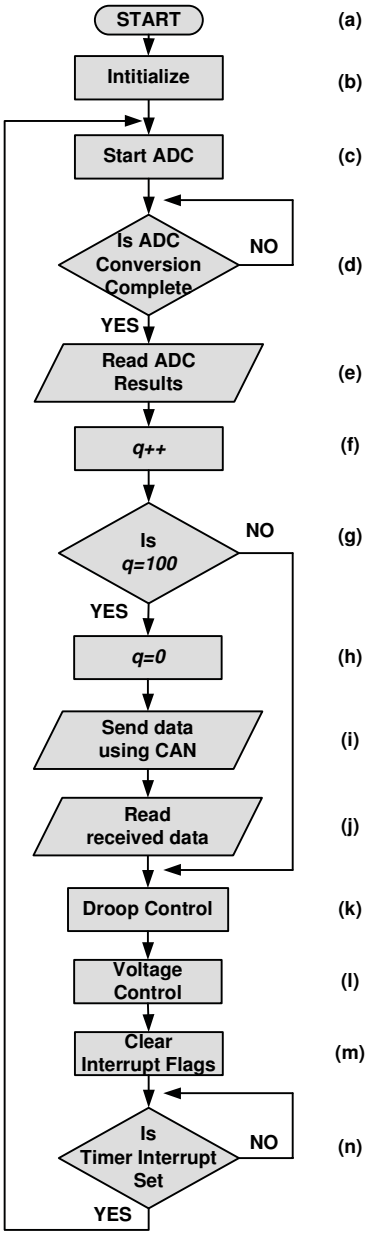

Figure 18: Flow chart of the proposed control scheme.

transceiver, SN65HVD235 is used to connect each converter to the CAN bus. Flow chart of the firmware used to realize the proposed scheme is shown in Fig. 18. In step-(b), the controller and CAN are initialized. CAN bus speed is set at 100kbps and timer period of TMS320F28335 is set at 100μs. When "timer counter" equals to the period value of timer, "timer interrupt" signal is generated and ADC conversion is initiated in step-(c). When ADC conversion is complete, ADC result registers are read, as given in step-(d) and step-(e). During step-(i) and step-(j) average current value of the source is communicated to other sources. These steps are executed once in every 100 interrupts (10ms). This corresponds to data communication rate of 100x2x8bps (1.6kbps) per source. In step-(k) and step-(l), droop and voltage controllers shown in Fig. 15

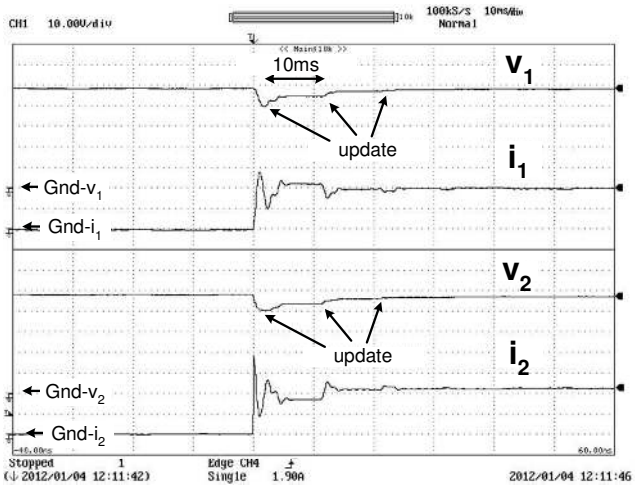

Figure 19: Experimentally obtained transient response for the proposed controller. Trace-1: Source-1 voltage (10V/div) and current (2A/div); Trace-2: Source-2 voltage (10V/div) and current (2A/div); X-axis: 10ms/div

are realized.

Each converter sends its load current information at every 10ms to other converters. Shift in voltage, Δv_j^0 is calculated by the controller using (3) and (4) at every 10ms. Droop and shift gains are set at 1.9Ω and 1.8Ω respectively. Fig. 19 shows the transient results for step change in load-2 from zero to full-load (8.44A). At the instant of turning on of the load, system voltage drops momentarily. However, within 25ms source-1 and 2 voltages settle to 48.57V and 47.90V respectively, which corresponds to the system voltage regulation of 1.2%. The instants of update in the voltage shift values, occur at every 10ms as shown in Fig. 19. Currents supplied by source-1 and source-2 are found to be 3.94A and 4.50A respectively. Deviation in source current from the ideal value is 6.6%.

For both controllers, voltage regulation is less than 5%. Deviation in load sharing for the proposed scheme (6.6%) is much smaller than that for droop method (35.8%). This confirms the effectiveness of the proposed scheme to reduce current deviation and achieve equal sharing of load.

4.3 Fail-safe Behavior of The Proposed Scheme

A key advantage of the decentralized scheme, proposed in this paper is high reliability. To substantiate this claim, a three source dc microgrid prototype is developed. Schematic of the developed system is shown in Fig. 20.

Each source is a dc-dc buck converter, as shown in Fig. 15. The proposed decentralized

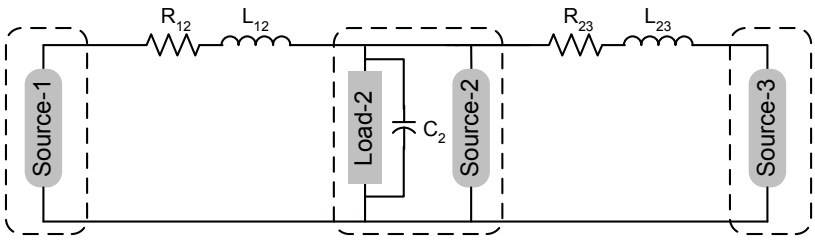

Figure 20: A three source dc microgrid

Table 4: Interconnecting cable parameters

Parameters	**Values**
R_{12}	205mΩ
L_{12}	463μH
R_{23}	192mΩ
L_{23}	434μH

control scheme using CAN is realized in all the sources. Interconnecting cable parameters are given in Table-4 and source parameters are the same as given in Table-1. At steady state, load voltage is 48V and current supplied by source 1, 2 and 3 are 2.63A, 3.15A and 2.68A respectively. The maximum deviation in source currents from their ideal value is 11.7%. The system is on partial load. If one source malfunctions, power capacity of other two sources is sufficient to supply the load. Failure of source-3 is emulated by removing the auxiliary (control) power supply of source-3. Load voltage and source currents during this disturbance are shown in Fig. 21. At steady state the load voltage is maintained at 47V. Source currents reach steady state in about 20ms. Currents supplied by source 1 and 2 are 3.86A and 4.45A respectively. This corresponds to current sharing error of about 7.1%. This confirms that the system is capable of operation even during failure of source-3.

Since source-2 is directly connected to the load, failure of source-2 is also studied. In this case, fault is emulated in source-2 instead of source-3 and the results are shown in Fig. 22. Load voltage after the fault is maintained at 46.63V. This corresponds to load voltage regulation of 2.85%. Currents supplied by source 1 and 3 are 4.11A and 4.15A respectively. This corresponds to current sharing error less than 0.5%. This confirms satisfactory steady state and transient performance of the proposed scheme during source malfunction.

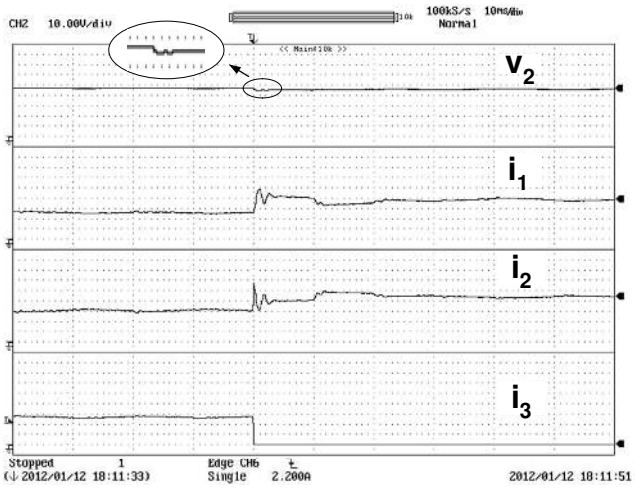

Figure 21: Experimentally obtained transient response for fault in source-3. Trace-1: Load voltage (10V/div), Trace-2: Source-1 current (2A/div), Trace-3: Source-2 current (2A/div), Trace-4: Source-3 current (2A/div); X-axis: 10ms/div

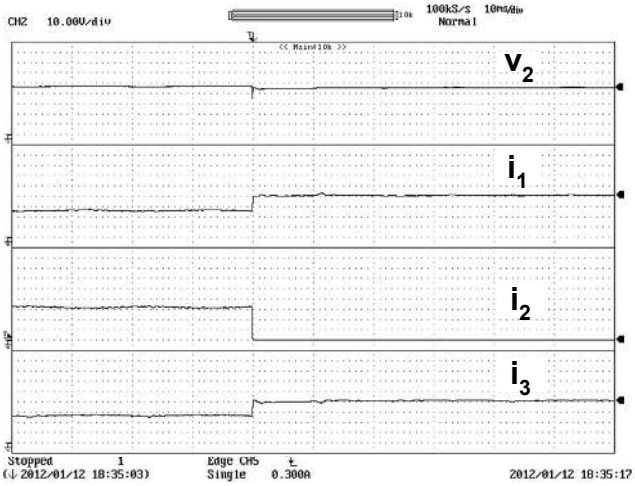

Figure 22: Experimentally obtained transient response for fault in source-2. Trace-1: Load voltage (10V/div), Trace-2: Source-1 current (2A/div), Trace-3: Source-2 current (2A/div), Trace-4: Source-3 current (2A/div); X-axis: 10ms/div

5 Conclusion

The paper presents a distributed control suitable for dc microgrid systems. As opposed to the conventional hierarchical control approach, it does not require a central controller. The control is based on the droop control method together with a decentralized average current sharing control. The droop control is a local controller which does not require any communication system, achieves good current sharing at the expense of compromising the voltage regulation. Further, the voltage is not constat in the microgrid. Therefore, the current sharing is hard to achieve when the distance between the sources is considerable. In order to improve this drawback another loop has been implemented, which uses low bandwidth digital communication between

the sources. It is based on averaging the total current supplied by the sources. To verify the effectiveness of the scheme, simulation study is carried out. Further, to confirm the viability of the scheme, experimental studies are conducted on a laboratory prototype developed for the purpose. Results obtained prove that improved performance is obtained by using the proposed scheme than that with droop controller.

APPENDIX

A Modeling of DC Microgrid

Voltage controller is assumed to be much faster than droop controller. Hence, while analyzing the microgrid structure with droop controllers, fast dynamics are neglected by assuming the output voltage, v_j equal to its reference value, v_j^{ref}. The proposed controller derives the reference voltage using the source current. Control equation for source-j is as follows:

$$v_j = v_j^0 + \Delta v_j^0 - d_j i_j \tag{15}$$

In matrix form, droop equations for all the sources are written as follows:

$$\mathbf{v} = \mathbf{v^0} + \mathbf{\Delta v^0} - \mathbf{D i} \tag{16}$$

where, $\mathbf{v}$, $\mathbf{v^0}$, $\mathbf{\Delta v^0}$ and $\mathbf{i}$ are column vectors of n dimension and $\mathbf{D}$ is diagonal matrix of $n \times n$ dimension. Sampling and updating of the voltage shift, $\mathbf{\Delta v^0}$ is much slower than the droop controller. Therefore, dynamics associated with voltage shift are neglected. Applying small signal analysis,

$$\hat{\mathbf{v}} = -\mathbf{D}\hat{\mathbf{i}} \tag{17}$$

where, $\hat{(\,)}$ represents the small signal variation around the point of operation.

Power consumed by load-j, p_{Lj} is given by the following equation.

$$v_j i_{Lj} = p_{Lj} \tag{18}$$

where, i_{Lj} is the load current of node-j. Small signal equation representing load-j is,

$$V_j\hat{i}_{Lj} + I_{Lj}\hat{v_j} = \hat{p}_{Lj} \tag{19}$$

where, V_j and I_{Lj} are the steady state values of voltage and load current of node-j respectively. Writing load equation in matrix form,

$$\mathbf{V}\hat{\mathbf{i}}_{\mathbf{L}} + \mathbf{I_L}\hat{\mathbf{v}} = \hat{\mathbf{p}}_{\mathbf{L}} \tag{20}$$

where, $\hat{\mathbf{i}}_{\mathbf{L}}$ & $\hat{\mathbf{p}}_{\mathbf{L}}$ are column vectors of n dimension and $\mathbf{V}$ & $\mathbf{I_L}$ are diagonal matrix of $n \times n$ dimension.

Interconnecting cable is modeled as series combination of resistance and inductance. Equation for cable is written as:

$$v_{jk} = l_{jk}\frac{di_{jk}}{dt} + r_{jk}i_{jk} \tag{21}$$

Combining all cable equations in matrix form:

$$\mathbf{v_{xy}} = \mathbf{L}\frac{d\mathbf{i_{xy}}}{dt} + \mathbf{R}\mathbf{i_{xy}} \tag{22}$$

where $\mathbf{R}$ and $\mathbf{L}$ are diagonal matrices of $m \times m$ dimension. Writing the small signal equivalent equation gives,

$$\hat{\mathbf{v}}_{\mathbf{xy}} = \mathbf{L}\frac{d\hat{\mathbf{i}}_{\mathbf{xy}}}{dt} + \mathbf{R}\hat{\mathbf{i}}_{\mathbf{xy}} \tag{23}$$

Writing equation for load capacitors in matrix form,

$$\hat{\mathbf{i}}_{\mathbf{c}} = \mathbf{C}\frac{d\hat{\mathbf{v}}}{dt} \tag{24}$$

where, $\hat{\mathbf{i}}_{\mathbf{c}}$ is the column vectors of n dimension and $\mathbf{C}$ is diagonal matrix of $n \times n$ dimension.

Interconnection structure of the system is expressed by the Kirchhoff's Voltage Law (KVL) and Kirchhoff's Current Law (KCL) of network. In matrix form, KVL is given below:

$$\hat{\mathbf{v}}_{\mathbf{xy}} = \mathbf{M}\hat{\mathbf{v}} \tag{25}$$

where, $\mathbf{M}$ is the incidence matrix of $m \times n$ dimension. It consists of -1, 0 and +1 such that row corresponding to branch-jk has +1 at j^{th} column, -1 at k^{th} column and 0 at remaining entries of the row. In matrix form, KCL is given below:

$$\hat{\mathbf{i}} - \hat{\mathbf{i}}_{\mathbf{L}} - \hat{\mathbf{i}}_{\mathbf{c}} = \mathbf{M}^{\mathbf{T}} \hat{\mathbf{i}}_{\mathbf{xy}} \tag{26}$$

where, $(\ )^{\mathbf{T}}$ is the transpose of matrix.

Linearized small signal equations of the different components of the system are given by (17), (20), (23), (24), (25) and (26). Resulting equivalent system model, integrating these system components, is given by (9)-(13). $\mathbf{N_{mxn}}$ is a zero matrix.

References

[1] S. Anand and B.G. Fernandes, "Optimal Voltage Level for DC Microgrids," *36th Annu. IEEE Ind. Electron. Society Conf., IECON'2010*, pp.3034-3039, Nov 2010

[2] S. Anand and B.G. Fernandes, "Steady state performance analysis for load sharing in DC distributed generation system," *10th Int. Conf. on Environment and Electrical Engineering, EEEIC'2011*, pp.1-4, May 2011

[3] D. Salomonsson, L. Soder and A. Sannino, "An Adaptive Control System for a DC Microgrid for Data Centers," *IEEE Trans. Ind. Appl.*, vol.44, no.6, pp.1910-1917, 2008

[4] H. Kakigano, Y. Miura and T. Ise, "Low-Voltage Bipolar-Type DC Microgrid for Super High Quality Distribution," *IEEE Trans. Power Electron.*, vol.25, no.12, pp.3066-3075, Dec. 2010

[5] Tsai-Fu Wu, Kun-Han Sun, Chia-Ling Kuo and Chih-Hao Chang, "Predictive Current Controlled 5-kW Single-Phase Bidirectional Inverter With Wide Inductance Variation for DC-Microgrid Applications," *IEEE Trans. Power Electron.*, vol.25, no.12, pp.3076-3084, Dec. 2010

[6] A. Kwasinski, "Quantitative Evaluation of DC Microgrids Availability: Effects of System Architecture and Converter Topology Design Choices," *IEEE Trans. Power Electron.*, vol.26, no.3, pp.835-851, March 2011

[7] Yuan-Chih Chang and Chang-Ming Liaw, "Establishment of a Switched-Reluctance Generator-Based Common DC Microgrid System," *IEEE Trans. Power Electron.*, vol.26, no.9, pp.2512-2527, Sept. 2011

[8] J. M. Guerrero, J.C. Vasquez, J. Matas, L.G. de Vicuna and M. Castilla, "Hierarchical Control of Droop-Controlled AC and DC Microgrids-A General Approach Toward Standardization," *IEEE Trans. Ind. Electron.*, vol.58, no.1, pp.158-172, Jan. 2011

[9] R. Majumder, G. Ledwich, A. Ghosh, S. Chakrabarti and F. Zare, "Droop Control of Converter-Interfaced Microsources in Rural Distributed Generation," *IEEE Trans. Power Delivery*, vol.25, no.4, pp.2768-2778, Oct. 2010

[10] D. Guezgouz, D.E. Chariag, Y. Raingeaud and J.-C. Le Bunetel, "Modeling of Electromagnetic Interference and PLC Transmission for Loads Shedding in a Microgrid," *IEEE Trans. Power Electron.*, vol.26, no.3, pp.747-754, March 2011

[11] A. Pinomaa, J. Ahola and A. Kosonen, "Power-line communication-based network architecture for LVDC distribution system," *IEEE International Symposium on Power Line Communications and Its Applications, ISPLC'2011*, pp.358-363, April 2011

[12] J. Anatory, N. Theethayi, R. Thottappillil, M.M. Kissaka and N.H. Mvungi, "The Influence of Load Impedance, Line Length, and Branches on Underground Cable Power-Line Communications (PLC) Systems," *IEEE Trans. Power Del.*, vol.23, no.1, pp.180-187, Jan. 2008

[13] Yao Zhang and Hao Ma, "Theoretical and Experimental Investigation of Networked Control for Parallel Operation of Inverters," *IEEE Trans. Ind. Electron.*, vol.59, no.4, pp.1961-1970, April 2012

[14] Chien-Liang Chen, Yubin Wang, Jih-Sheng Lai, Yuang-Shung Lee and D. Martin, "Design of Parallel Inverters for Smooth Mode Transfer Microgrid Applications," *IEEE Trans. Power Electron.*, vol.25, no.1, pp.6-15, Jan. 2010

[15] M.P. Kazmierkowski and L. Malesani, "Current control techniques for three-phase voltage-source PWM converters: a survey," *IEEE Trans. Ind. Electron.*, vol.45, no.5, pp.691-703, Oct 1998

[16] H.-H. Huang, C.-Y. Hsieh, J.-Y. Liao and K.-H. Chen, "Adaptive Droop Resistance Technique for Adaptive Voltage Positioning in Boost DCDC Converters," *IEEE Trans. Power Electron.*, vol.26, no.7, pp.1920-1932, July 2011

[17] C. Yuen, A. Oudalov and A. Timbus, "The Provision of Frequency Control Reserves From Multiple Microgrids," *IEEE Trans. Ind. Electron.*, vol.58, no.1, pp.173-183, Jan. 2011

[18] E. Barklund, N. Pogaku, M. Prodanovic, C. Hernandez-Aramburo and T.C. Green, "Energy Management in Autonomous Microgrid Using Stability-Constrained Droop Control of Inverters," *IEEE Trans. Power Electron.*, vol.23, no.5, pp.2346-2352, Sept. 2008

[19] H. Kanchev, Di Lu, F. Colas, V. Lazarov and B. Francois, "Energy Management and Operational Planning of a Microgrid With a PV-Based Active Generator for Smart Grid Applications," *IEEE Trans. Ind. Electron.*, vol.58, no.10, pp.4583-4592, Oct. 2011

[20] Changsong Chen, Shanxu Duan, Tao Cai, Bangyin Liu and Guozhen Hu, "Optimal Allocation and Economic Analysis of Energy Storage System in Microgrids," *IEEE Trans. Power Electron.*, vol.26, no.10, pp.2762-2773, Oct. 2011

[21] B.K. Johnson, R.H. Lasseter, F.L. Alvarado and R. Adapa, "Expandable multiterminal DC systems based on voltage droop," *IEEE Trans. Power Del.*, vol.8, no.4, pp.1926-1932, Oct 1993

[22] He Zhang, F. Mollet, C. Saudemont and B. Robyns, "Experimental Validation of Energy Storage System Management Strategies for a Local DC Distribution System of More Electric Aircraft," *IEEE Trans. Ind. Electron.*, vol.57, no.12, pp.3905-3916, Dec. 2010

[23] P. Karlsson and J. Svensson, "DC bus voltage control for a distributed power system," *IEEE Trans. Power Electron.*, vol.18, no.6, pp. 1405- 1412, Nov. 2003

[24] J. Schonberger, R. Duke and S.D. Round, "DC-Bus Signaling: A Distributed Control Strategy for a Hybrid Renewable Nanogrid," *IEEE Trans. Ind. Electron.*, vol.53, no.5, pp.1453-1460, Oct. 2006

[25] Li Zhang, Tianjin Wu, Yan Xing, Kai Sun and J.M. Gurrero, "Power control of DC microgrid using DC bus signaling," *26th Annual IEEE Applied Power Electronics Conf. and Expo., APEC'2011*, pp.1926-1932, March 2011

[26] Kai Sun, Li Zhang, Yan Xing and J.M. Guerrero, "A Distributed Control Strategy Based on DC Bus Signaling for Modular Photovoltaic Generation Systems With Battery Energy Storage," *IEEE Trans. Power Electron.*, vol.26, no.10, pp.3032-3045, Oct. 2011

[27] D.J. Perreault, Jr. R.L. Selders and J.G. Kassakian, "Frequency-based current-sharing techniques for paralleled power converters," *IEEE Trans. Power Electron.*, vol.13, no.4, pp.626-634, Jul 1998

[28] A. Tuladhar and H. Jin, "A novel control technique to operate DC/DC converters in parallel with no control interconnections," *29th Annual IEEE Power Electronics Specialists Conference, PESC'98*, vol.1, no., pp.892-898 vol.1, May 1998

[29] I. Batarseh, K. Siri and H. Lee, "Investigation of the output droop characteristics of parallel-connnected DC-DC converters," *25th IEEE Power Electronics Specialists Conference, PESC'94*, pp.1342-1351 vol.2, 20-25 Jun 1994

[30] Jung-Won Kim, Hang-Seok Choi and Bo Hyung Cho, "A novel droop method for converter parallel operation," *IEEE Trans. Power Electron.*, vol.17, no.1, pp.25-32, Jan 2002

[31] M. C. Chandorkar, D. M. Divan and R. Adapa, "Control of parallel connected inverters in standalone AC supply systems," *IEEE Trans. Ind. Appl.*, vol.29, no.1, pp.136-143, Jan/Feb 1993

[32] S. V. Iyer, M. N. Belur and M. C. Chandorkar, "A Generalized Computational Method to Determine Stability of a Multi Inverter Microgrid," *IEEE Trans. Power Electron.*, vol.25, no.9, pp.2420-2432, Sept. 2010

[33] N. Pogaku, M. Prodanovic and T. C. Green, "Modeling, Analysis and Testing of Autonomous Operation of an Inverter-Based Microgrid," *IEEE Trans. Power Electron.*, vol.22, no.2, pp.613-625, March 2007

[34] E. Serban and H. Serban, "A Control Strategy for a Distributed Power Generation Microgrid Application With Voltage- and Current-Controlled Source Converter," *IEEE Trans. Power Electron.*, vol.25, no.12, pp.2981-2992, Dec. 2010

[35] Jaehong Kim, J.M. Guerrero, P. Rodriguez, R. Teodorescu and Kwanghee Nam, "Mode Adaptive Droop Control With Virtual Output Impedances for an Inverter-Based Flexible AC Microgrid," *IEEE Trans. Power Electron.*, vol.26, no.3, pp.689-701, March 2011

[36] A. Tuladhar, H. Jin, T. Unger and K. Mauch, "Parallel operation of single phase inverter modules with no control interconnections," *12th Annual Applied Power Electronics Conference and Exposition, APEC '97*, vol.1, no., pp.94-100, Feb 1997

[37] A. Tuladhar, Hua Jin, T. Unger and K. Mauch, "Control of parallel inverters in distributed AC power systems with consideration of line impedance effect," *IEEE Trans. Ind. Appli.*, vol.36, no.1, pp.131-138, Jan/Feb 2000

[38] Weihong Qiu and Zhixiang Liang, "Practical design considerations of current sharing control for parallel VRM applications," *20th Annual Applied Power Electronics Conference and Exposition, APEC'2005*, vol.1, pp.281-286, March 2005